

# Study on development of vessel for shock pressure treatment for food

**Masahiko Otsuka<sup>1</sup>, Hironori Maehara<sup>2</sup>, Mhamed Souli<sup>3</sup>, and Shigeru Itoh<sup>2</sup>)**

<sup>1</sup>Graduate school of Science and Technology, Kumamoto University  
2-39-1 Kurokami, Kumamoto 860-8555, Japan  
masahiko@shock.smrc.kumamoto-u.ac.jp

<sup>2</sup>Shock Wave and Condensed Matter Research Center, Kumamoto University  
2-39-1 Kurokami, Kumamoto 860-8555, Japan  
maehara@shock.smrc.kumamoto-u.ac.jp  
itoh@mech.kumamoto-u.ac.jp

<sup>3</sup>University of Science and Technology of Lille  
UMR CNRS 8107, Avenue Paul Langevin 59655 Villeneuve d'Ascq cedex, France  
mhamed.souli@univ-lille1.fr

## ABSTRACT

In recent years, the food processing using high-energy pressure pulse is gaining attention due to no heat evolution in the process. In this study a vessel was designed for the shock pressure treatment of food. An underwater shock wave generated by the detonating fuse was applied as the source of high-energy pressure pulse. The underwater shock wave was investigated by optical observation and pressure measurement experiments. The results are then compared with the computer simulation using LS-DYNA code. The agreement between the experimental results and the numerical analysis is found to be good. The food processing of apple was performed using the designed vessel. The hardness of the apple has decreased showing the effectiveness of the newly designed vessel.

## 1. INTRODUCTION

Stabilizers and additives are added to food to preserve flavor or improve its taste and appearance. However, recent literature reports that these additives affect human body and many nutritional compounds are lost by the excessive use of antiseptics. Hence, food processing requires food safety and retention of nutritional value. In the conventional food processing, more energy and time is required for applying antiseptics, extract useful nutritional compounds and for seasoning foods. A viable technique for food processing using an underwater shock wave is proposed in this paper. In this technique, extraction and softening of food can be performed at low temperature and short time by applying underwater shock wave, which can also do the sterilization<sup>1)-3)</sup>. As the process requires limited steps and less time, it is an efficient method for food processing. It was demonstrated that extraction of polyphenolic compounds increased in the apple juice processed by

underwater shock wave<sup>4</sup>). This processing is useful for the extraction of juice and nutritional compounds. The design and evaluation of a pressure vessel to perform such a food processing using high-pressure is indispensable.

In this study, underwater shock wave is generated by underwater explosion of a detonating fuse. When an underwater shock wave passes through the food, it causes the softening of food by the incident wave and the difference of the impedance in food.

In this study, as a first step, the propagation process and the attenuation of the underwater shock wave generated by underwater explosion of detonating fuse were investigated by optical observation and pressure measurement. Secondly, a food-processing vessel, which consists of a detonating fuse, water, silicon rubber and stainless steel (JIS SUS304), was designed and manufactured. This vessel was evaluated by numerical analysis using LS-DYNA code<sup>5</sup>) and the relation between the experimental results and the numerical results of underwater shock wave generated by the detonating fuse was analyzed. Such a numerical analysis is good for saving the cost for designing the pressure vessel. Finally, the food processing using apple was done using the designed vessel and the performance of this vessel was evaluated.

## 2. TRANSMISSION AND REFLECTION OF SHOCK WAVE

A shock wave consists, ideally, of a shock front, a flat top, and a release part<sup>6</sup>). The schematic illustration of the transmission and reflection of a shock wave is shown in Fig. 1. Now, a shock wave propagated through medium A is applied to medium B. The incident shock wave by the velocity of  $U_i^s$  propagates to the boundary of medium A and medium B. When the incident wave reflects on this boundary, the incident wave converts into a transmitted wave and a reflected wave. The equations of conservation of momentum for the transmitted wave and the reflected wave are shown below.

$$P^i - P_0 = \rho_A U_s^i u_p^i \quad (1)$$

$$P^i - P_0 = \rho_A U_s^i u_p^i \quad (2)$$

where  $i$  and  $t$  superscripts represent the incident wave and the transmitted wave, respectively.  $\rho_A$  and  $\rho_B$  show the initial density of medium A and medium B, respectively. Since the shock impedance is dependent the incident pressure, the incident shock impedance  $\rho_A U_s^i$  and the reflected shock impedance  $\rho_A^r U_s^r$  are equal.

$$\rho_A U_s^i = \rho_A^r U_s^r \quad (3)$$

Consequently, the equation of momentum conservation for the reflected wave will be as follows.

$$P^r - P^i = \rho_A^r U_s^r (u_p^r - u_p^i) = \rho_A U_s^i (u_p^r - u_p^i) \quad (4)$$

By assumption of continuity, the reflected pressure  $P^r$  and the particle velocity  $u_p^r$  can be found as  $P^r = P^i$  and  $u_p^r = u_p^i$ . Similarly the pressure of the transmitted shock wave in medium B can be shown as follows.

$$P' = \rho_0^B U_s^t u_p' = \rho_0^B (c^B + s^B u_p^t) u_p' \quad (5)$$

where  $C^B$  and  $s^B$  are the sonic wave velocity and Hugoniot parameter<sup>7)</sup> in medium B, respectively. In view of eqs.(1) and (5),  $P_0$  can be neglected in comparison with  $P_i$  and  $P_r$ , then the  $P_r$  is written as

$$P^r = P^t = \frac{2\rho_B U_s^t}{\rho_A U_s^i + \rho_B U_s^t} P^i \quad (6)$$

When a shock wave traveling in the low impedance medium A arrives at the boundary with the high impedance medium B, transmitted and reflected waves propagate as shock waves. On the other hand, a shock wave propagates in high impedance medium A reaches the boundary with low impedance medium B, produces a transmitted shock wave and a reflected expansion wave.

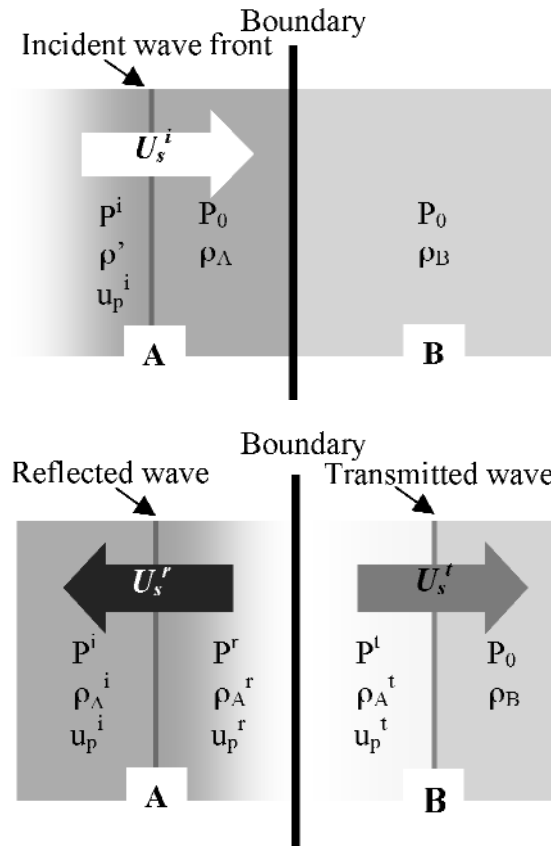


Figure 1 Schematic illustration for incidence, reflection, and transmission of a shock wave in different media

It is reported that underwater shock wave can be employed for improvement of wood properties<sup>8)</sup>. The underwater shock wave applied on wood, the shock wave and the reflected wave propagated to cell into wood destruct the cell of wood. Such a treatment has resulted in better dryability character and moreover enhanced permeability of wood which is importance in preparation of fireproof wooden materials by the diffusing fireproof chemicals into the wood. In this study, when an underwater shock wave passes through the food, the food processing is achieved by the incident shock wave and the reflected wave produced by the impedance difference of food, water and vessel.

### 3. EXPERIMENTAL METHOD

Detonating fuse (NIPPON KAYAKU Co., Ltd.) was used as the high pressure source for the food processing. Detonating fuse is a high velocity non-electric blasting, flexible, easy to use and extremely safe accessory. Detonating fuse has a core of pentaerythritoltetranitrate (PETN) covered with various layers of cotton and synthetic fibers. The density of PETN in the detonating fuse is 1200kg/m<sup>3</sup>, the diameter of fuse is 5.4mm, and the linear density of the explosive charge is 10g/m. This explosive has a detonation velocity of 6300m/s. The underwater shock wave generated by the underwater explosion of the detonating fuse was measured by the optical observation and the pressure measurement. The experimental setup for optical observation is shown in Fig. 2. This fuse was initiated by No.6 electric detonator (ASAHI KASEI Chemicals Co.) in water.

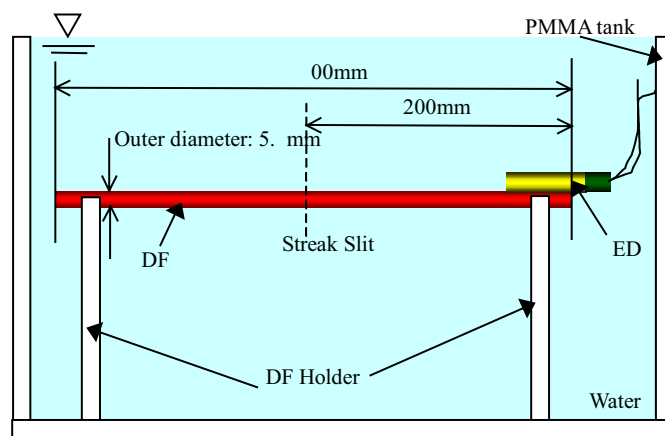
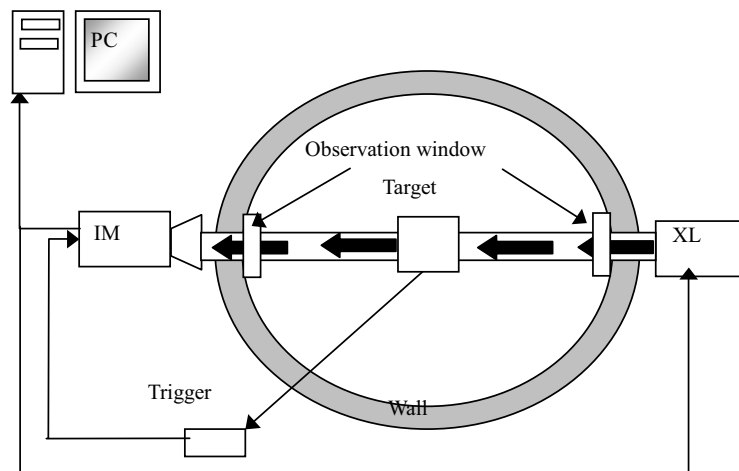


Figure 2 Experimental setup for optical observation

The optical observation that is based on shadowgraphy was used to evaluate the underwater shock wave generated by the detonation fuse. The shadowgraph system used in this study is shown in Fig. 3. In this system the shadow of the light is observed and projected by density change on a screen or the film of the camera. The shadowgraph method has been used for visualization of a shock wave or the motion of a wave for many years. The shadowgraph system and a high-speed camera (IMACON468 of HADLAND PHOTONICS, Framing rate; 100 to 100000000 fps, Streak window; 10ns to 100μs) were used to observe the underwater shock wave. Framing photographs and streak photograph for the underwater shock wave generated by the detonating fuse are taken by a high-speed camera.



PC; Imaging Processing Software

IM; High-Speed Camera

XL; Xenon Flash Lamp

Figure 3 Shadowgraph system for optical observation

The pressure measurement of underwater shock wave was performed by the pressure transducer using the elastic bar to which two semiconductor strain gauges are connected<sup>9)</sup>. The feature of this pressure transducer is its capability to measure a pressure of about 1GPa for several times. The schematic drawing of the pressure transducer is shown in Fig. 4. This transducer consists of an elastic bar, which receives the pressure as underwater shock wave, a protective cap (JIS SKD11, 18mm in the outside diameter), and a protective stainless steel pipe (JIS SUS304, 18mm in the outside diameter, and 3mm in thickness). The elastic bar is a tungsten bar of 5mm in diameter and 300mm in length (0.2% yield stress 1.4GPa, dynamic Young's modulus 412.7GPa and characteristic frequency 500kHz). In this tungsten bar, two semiconductor strain gauges (Kyowa Electric Instrument Co., Ltd., 1mm in the gage length, resistance 350Ω, maximum strain  $3000 \times 10^{-6}$  and gauge factors 151) are fixed at a distance of 30 mm from the pressure-receiving end. The Wheat Stone bridge circuit is connected to these semiconductor gauges and a dummy gauge kept near the bar. The elastic stress wave propagates through the bar when an underwater shock wave is received at the end of the bar and a potential difference is caused in the bridge circuit by the generated stress. This potential difference is directly recorded to an oscilloscope without the amplifier.

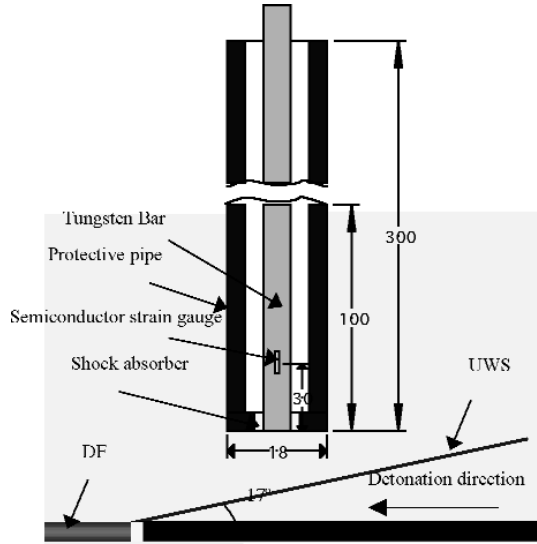


Figure 4 Schematic drawing of pressure transducer

Having the elastic stress generated in the bar  $P_B$ , Young's modulus  $E$ , the strain  $\epsilon$ , the sound velocity of tungsten bar  $C_B$  (4650m/s) and the density of the tungsten bar  $\rho_B$  (19088kg/m<sup>3</sup>) are given, it could be shown that  $E=C_B^2 \rho_B$  and  $P_B=E\epsilon$ . The gauge factor  $G$  can be obtained from  $G = \Delta R/R\epsilon$ . Having  $V_{out} = \frac{G \cdot \epsilon}{2} \cdot V_0$  and  $P_B=E\epsilon$ , the elastic stress in the bar can be expressed as

$$P_B = \frac{2E}{G \cdot V_0} \cdot K_1 \cdot V_{out} \quad (7)$$

where the value of the constant  $K_1$  is 1.173,  $G$  is 151,  $V_0$  is the circuit voltage and  $V_{out}$  is the output voltage. The Wheat Stone bridge circuit is shown in Fig. 5.

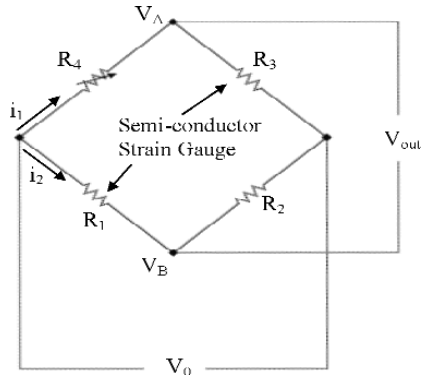


Figure 5 Wheat Stone bridge

Since the conservation of mass and momentum are applied on the boundary of water and a tungsten bar, the peak pressure on the surface of the bar is obtained from the following equations by matching the acoustic impedance in water and tungsten bar.

$$P_w = \frac{1 + \frac{\rho_w \cdot C_w}{\rho_B \cdot C_B} \cdot \cos \alpha}{1 + \cos^2 \alpha} \cdot P_B \cdot K_2 \quad (8)$$

where  $\rho_w$  is the density of water (1000kg/m<sup>3</sup>) and  $C_w$  is the sound velocity of water (1490m/s). Also, the value of the constant  $K_2$  is 1.4. When the incident angle is  $\alpha=0^\circ$ , the Eq. (8) is shown as follows.

$$P_w = \frac{\rho_B \cdot C_B + \rho_w \cdot C_w}{2\rho_B \cdot C_B} \cdot P_B \cdot K_2 \quad (9)$$

The underwater shock wave generated by the detonating fuse is applied to a tungsten bar at the angle of 17° from the results of the optical observation.

Processing of an apple was performed by the designed pressure vessel. The processing effect was evaluated by measuring the hardness of the apple. Hardness was measured before and after processing by vertically pushing down a DUROMETER (TECLOCK Co.) with a constant speed against the surface of the apple. The weight of the durometer placed on the apple was acting as the measuring force.

#### 4. NUMERICAL ANALYSIS METHOD

The propagation of the underwater shock wave, the detonation of detonating fuse, and the vessel are evaluated by the numerical analysis. The vessel for food processing is designed by detonating fuse, water, silicon rubber and SUS304. In numerical analysis, food is not arranged, and only the layer of water is arranged. The numerical analysis model is shown in Fig. 6. The mesh size was 1x1mm.

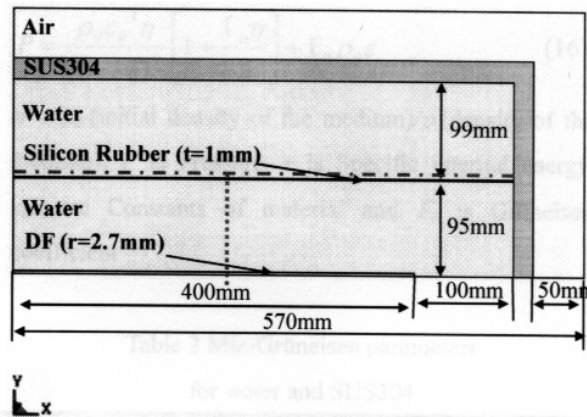


Figure 6 Numerical analysis model

This vessel is simulated with fluid and structure coupling algorithm<sup>10,11)</sup> and the multi-material formulation of LS-DYNA3D. The fluid is solved by using an Eulerian formulation on a Cartesian grid that overlaps the structure, while the structure is described by a Lagrangian approach. The Eulerian formulation is used for the detonation product of explosive, water and air, and the Lagrangian method is used for rubber and SUS304 in this study. In the pure Lagrangian approach, the mesh moves with the material, making it easy to track surfaces and apply boundary conditions. Using an Eulerian description, the mesh remains fixed while the material passes through it. In fluid-structure interaction, contact algorithms compute interface forces due to impact of the structure on the fluid. These forces are applied to the fluid and structure nodes in contact in order to prevent node from passing through contact interface. The governing equations for the fluid formulation are given by conservation equation of:

(i) The equation of mass conservation

$$\frac{\partial \rho}{\partial t} = -\rho \cdot \text{div}(\mathbf{v}) - v_i \frac{\partial \rho}{\partial x_i} \quad (10)$$

(ii) The equation of momentum conservation

$$\rho \frac{\partial v_i}{\partial t} = \sigma_{ij,j} - \rho \cdot v_i \frac{\partial v_i}{\partial x_j} \quad (11)$$

(iii) The equation of energy conservation

$$\rho \frac{\partial e}{\partial t} = \sigma_{ij} \cdot \varepsilon_{ij} - \rho \cdot v_i \frac{\partial e}{\partial x_j} \quad (12)$$

The governing equations for the structure formulation are given by:

(i) The equation of momentum conservation

$$\rho \frac{\partial v_i}{\partial t} = \sigma_{ij,n} \quad (13)$$

(ii) The equation of energy conservation

$$\rho \frac{\partial e}{\partial t} = \sigma_{ij} \cdot \varepsilon_{ij} \quad (14)$$

where  $\rho$  is the density,  $\sigma$  is the Cauchy stress, and  $\mathbf{v}$  is the velocity of fluid. In Lagrangian formulation, the mass is automatically conserved. In LS-DYNA, a viscosity term is not considered in Lagrangian formulation and Eulerian formulation.

Jones-Wilkins-Lee (JWL) equation of state<sup>12,13)</sup> for detonation product gas of the detonating fuse and Mie-Gruneisen equation of state for water and SUS304 is used in the



model, because a hydrodynamic material model requires an equation of state to define the pressure-volume relationship.

JWL equation is used for the equation of state for the detonating fuse. This equation is shown below (15) and the parameters are shown in Table 1.

$$P_{JWL} = A \left[ 1 - \frac{\omega}{VR_1} \right] \exp(-R_1 V) + B \left[ 1 - \frac{\omega}{VR_2} \right] \exp(-R_2 V) + \frac{\omega e}{V} \quad (15)$$

$V = \rho_0$  (Initial density of an explosive)/ $\rho$  (Density of detonation gas),  $P_{JWL}$  is pressure,  $e$  is Specific internal energy and  $A, B, R_1, R_2$  and  $\omega$  are JWL parameters.

Table 1 JWL parameter for detonating fuse

	A (GPa)	B (GPa)	R1	R2	$\omega$
DF	452.35	8.85	5.485	1.425	0.28

The Grüneisen equation is used for the equation of state of water and SUS304. Equation (16) gives Mie-Grüneisen equation in which the higher degree values are not taken into account. The values of the parameters are shown in Table 2.

$$P = \frac{\rho_0 c_0^2 \eta}{(1 - s\eta)^2} \left[ 1 - \frac{\Gamma_0 \eta}{2} \right] + \Gamma_0 \rho_0 e \quad (16)$$

$\eta = 1 - \rho_0$  (initial density of the medium)/ $\rho$  (density of the medium),  $P$  is Pressure,  $e$  is Specific internal energy,  $c_0, s$  are Constants of material and  $\Gamma_0$  is Grüneisen coefficient

Table 2 Mie-Grüneisen parameters for water and SUS304

	$\rho$ (kg/m <sup>3</sup> )	$c_0$ (m/s)	s	$\Gamma_0$
Water	1000	1490	1.79	1.65
SUS304	7900	4570	1.49	2.17

The equation of state for an air in this research was considered to be a Linear Polynomial equation<sup>5</sup>). This equation is shown below and each coefficient is shown in Table 3.

$$P = C_0 + C_1 \mu + C_2 \mu^2 + C_3 \mu^3 + (C_4 + C_5 \mu + C_6 \mu^2) E \quad (17)$$

The linear polynomial equation of state was used to model a gas with the gamma law equation of state. This may be achieved by setting.

$$C_0 = C_1 = C_2 = C_3 = C_6 = 0$$

and

$$C_4 = C_5 = \gamma - 1$$

where  $\gamma$  is ratio of specific heats.

Table 3 Linear polynomial parameter for air

	$\rho_0$ (kg/m <sup>3</sup> )	$\gamma$	C4	C5
Air	1.025	1.403	0.403	0.403

The elastic material is used for the silicon rubber. The density is 1230kg/m<sup>3</sup>, Young's modulus is 0.3MPa and Poisson's ratio is 0.48.

## 5. UNDERWATER SHOCK WAVE GENERATED BY DETONATING FUSE

Framing photographs of underwater shock wave generated by underwater explosion of the detonating fuse are shown in Fig. 7. It is evident from these framing photographs that the underwater shock wave propagates in an axially symmetric manner. The streak photograph represents the time in the horizontal positive axis and the distance in the vertical axis as shown in Fig. 8. In Fig. 7 and Fig. 8, DF shows the detonating fuse, UWS is underwater shock wave, and PG is the product gas produced by the detonation of the detonating fuse. The relation between the time and the distance of underwater shock wave obtained by the streak photograph is shown Fig. 9. The velocity of shock wave is shown by the inclination of this figure. The underwater shock wave generated from the detonating fuse attenuates while propagating in water. This inclination of a nonlinear curve represents attenuation of a shock wave. When the inclination becomes linear gradually, the shock wave converges.

The attenuation curve of the underwater shock pressure is shown in Fig. 10. This attenuation of an underwater shock wave is the curve expressed as  $P = 4870.8x^{-0.841}$ .

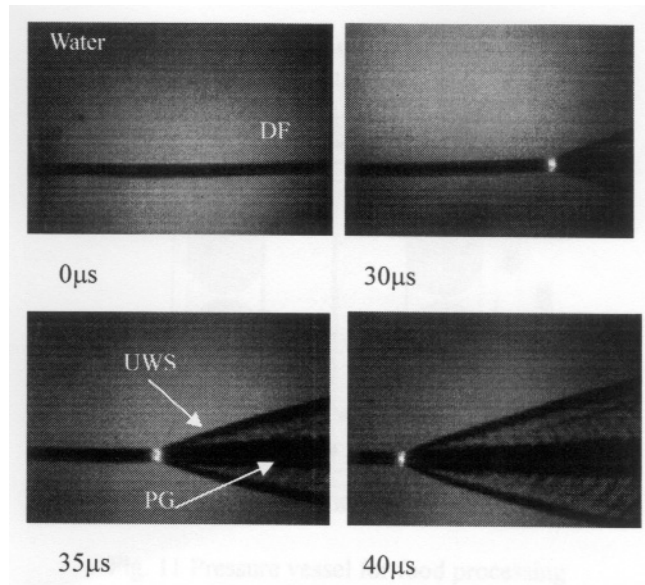


Figure 7 Framing photographs of underwater shock wave generated by underwater explosion of the detonating fuse

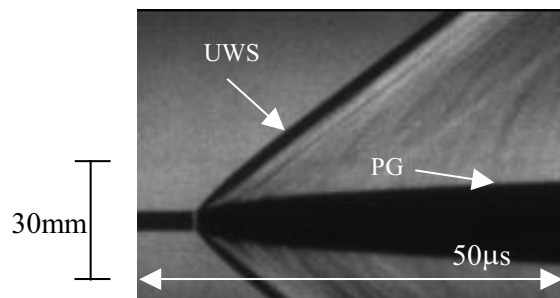


Figure 8 Streak photograph of underwater shock wave generated by underwater explosion of the detonating fuse

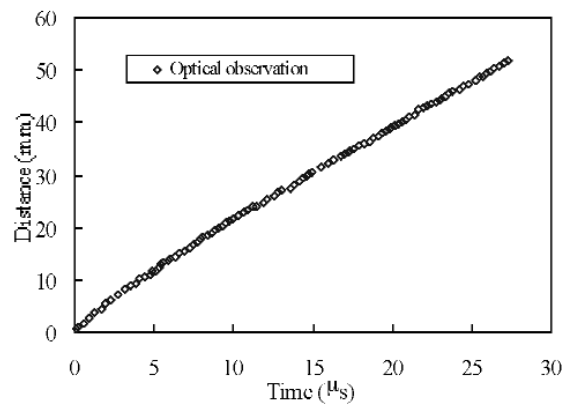


Figure 9 Relation between the time and the distance of underwater shock wave generated by the detonating fuse

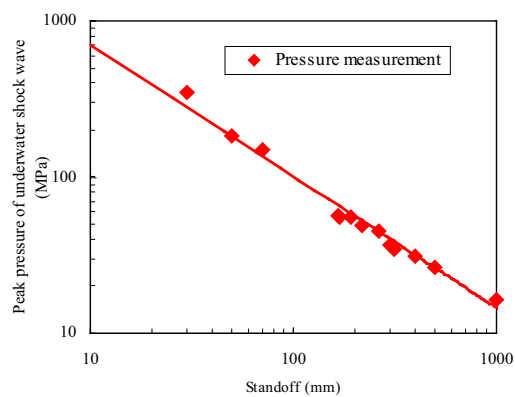


Figure 10 Attenuation curve of the pressure of the underwater shock wave

## 6. DESIGN OF VESSEL FOR FOOD PROCESSING

When food processing using an underwater shock wave is performed, it is known that the suitable pressure of underwater shock wave applied to food is  $30\sim70\text{MPa}^4$ ). The size of the designed pressure vessel was decided by an optical observation and the pressure measurements of the underwater shock wave generated by the detonating fuse. The schematic illustration of the food processing vessel is shown in Fig. 11, and the photograph of the designed pressure vessel and the setup in the vessel is shown in Fig. 12. ED shows the electric detonator. Since it must be used frequently, the pressure vessel is surrounded by SUS304, and the product gas of the detonation of the detonating fuse is prevented, from reaching the food, by the silicon rubber. Water around food is arranged in order to help propagation of a shock wave. Food is processed by the underwater shock wave passed through the silicon rubber and a reflected shock wave on SUS304.

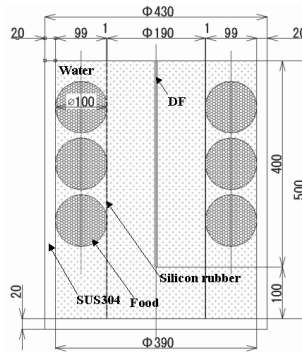


Figure 11 Pressure vessel for food processing

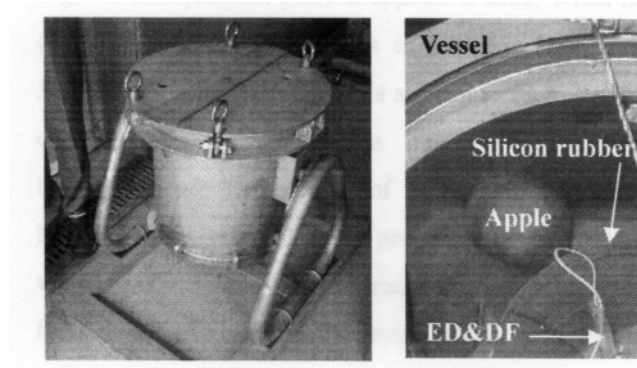


Figure 12 Photograph of pressure vessel and setup of apple in vessel

The pressure contours of the food processing vessel are shown in Fig. 13. The relation between the numerical results and the experimental results of underwater shock wave is shown in Table 4. The numerically obtained value of the underwater shock wave pressure at 200mm from the left end of calculation model shown by the dashed line in Fig. 6 is compared

with the experimental data. The agreement between the experimental result and the numerical analysis is found to be good. Moreover, the detonation velocity of the detonating fuse was 6069m/s in numerical analysis. The reflected wave between the water and the SUS304 is seen in the pressure contours at 320 $\mu$ s. Since the impedance of the SUS304 is higher in comparison with water, the reflected shock wave propagates as the shock wave. The duration of the pressure for the food processing in the vessel is increased by this reflection.

In numerical results, the pressure of the underwater shock wave passed through the silicon rubber was 49MPa. The reflected shock wave is over 49MPa from the results obtained by the pressure contours, but the food was not arranged in this model. Thus, the pressure value of the reflected shock wave applied on a food is not clarified. The particular value of reflected shock wave is still unclear and deserves further research.

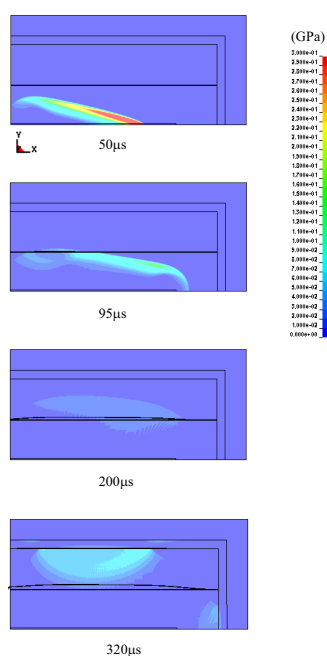


Figure 13 Pressure contours in the pressure vessel

Table 4 Relation between the numerical results and the experimental results of the underwater shock wave pressure on 200mm from left end of analysis model

Distance from DF (mm)	Numerical analysis (MPa)	Experiment (MPa)
30mm	289	279
50mm	186	181
70mm	125	137

Pressure histories of the underwater shock wave passed through the silicon rubber in

every 50mm (x direction) from left end on dashed-dotted line in Fig. 6 are shown in Fig. 14. This pressure pulse is applied to food. When the distance from the left end is in between 200mm to 300mm, the constant pressure is applied to food, but this constant pressure cannot be obtained around the beginning and terminating of the detonating fuse. However, the reflected wave propagates to the whole vessel (Fig. 13) and hence extraction and a softening of food are achieved by the underwater shock wave and the reflected wave.

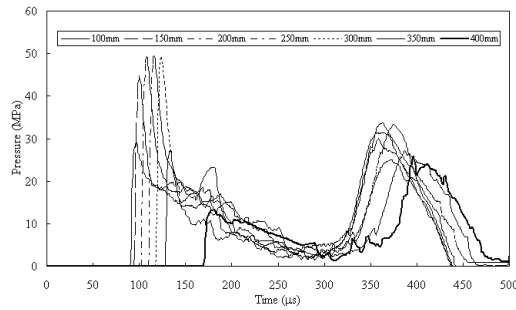


Figure 14 Pressure histories of the underwater shock wave applied on food

## 7. FOOD PROCESSING USING APPLE

The processing of apple was performed by using the designed vessel. A photograph of the apple before and after processing is shown in Fig. 15, and the hardness of apples is shown in Table 5. The hardness of apples was measured at the center of (3), near of the peel (1), and the in the middle of 3 and 1 (2). An apple does come apart by the shock wave, and almost retains its initial form. However, the hardness decreases at all measuring points. A juice by squeezing, without grating up, apples can be got. Furthermore, people not having biting ability, are able to take the food that was processed by this method.

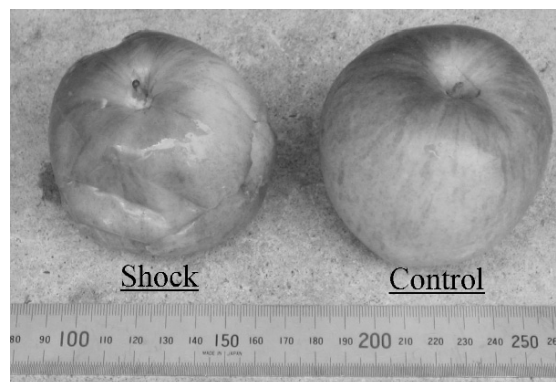



Figure 15 Photograph of apples before and after processing

Table 5 Hardness of the apple



Measurement point	1	2	3
Control	80	74	79
Shock	13	11	27

## 8. CONCLUSION

In this study, a pressure vessel for the food processing using detonating fuse was designed. This vessel was evaluated by experiments and numerical analysis. The agreement between experimental results and the numerical analysis of the underwater shock wave generated by the detonating fuse is found to be good. When the designed vessel was used, the incident underwater shock wave passed through the silicon rubber, and the reflected shock wave produced by the water and SUS304 is applied on the food. The pressure of the underwater shock wave propagating through silicone rubber was calculated to be 49MPa using numerical analysis. The processed apple became soft with reduced hardness and ready to use.

## ACKNOWLEDGEMENT

The support of the 21<sup>st</sup> Century COE program on Pulsed Power Science is gratefully acknowledged.

## REFERENCES

1. Acim M. Loske, Ulises M. Alvarez, Claudia Hernandez-Galcia, Eduardo Catano-Tostado, and Fernando E. Prieto, "Bactericidal effect of underwater shock waves on Escherichia coli ATOC 10536 suspensions" 2002, *Innovative Food Science & Emerging Technologies* 3, pp.321-327
2. Ulises M. Alvarez, Achim M. Loske, Eduardo Castano-Tostado, and Fernando E. Prieto, "Inactivation of Escherichia coli O157:H7, Salmonella Typhimurium and Listeria monocytogenes by underwater shock waves", 2004, *Innovative Food Science and Emerging Technologies* 5, pp.459-463
3. A. Takemoto, A. Oda, M. Iwahara, and S. Itoh, "On sterilization using the underwater shock wave under non-heating environment", *Proc. of 2006 ASME Pressure Vessels and Piping Conference*, ISBN 0-7918-3782-3, I749CD, 2006
4. A. Oda, T. Watanabe, and S. Itoh, "Basic study on pressure vessel for food processing by shock loading", *Proc. of 2006 ASME Pressure Vessels and Piping Conference*, ISBN 0-7918-3782-3, I749CD, 2006
5. J. O. Hallquist, "LS-DYNA Theoretical Manual", Livermore Software Technology Corporation, Livermore, 1998
6. M. A. Meyers, "Dynamic Behavior of Materials", A Wiley-Interscience Publication, New York, 1994, Chap. 7
7. S. P. Marsh, "LASL Shock Hugoniot Data", University of California Press, 1980
8. M. Nagahara, S. Matsumoto, and S. Itoh, "On shock loading the KARAMATSU wood for protecting the fire", *Proc. of Energetic technology in fluids, structures, and fluid-structure interactions*, PVP-Vol. 485-2, pp. 33-37, 2004
9. S. Itoh, S. Nagano, and M. Fujita, "The features of the Assembly for Punching of Pipes by Using the Converging Underwater Shock Wave", *Proceedings of the J.S.M.E.*, 1994, Vol.948-3
10. N. Aquelet, M. Souli, and L. Olovsson, "Euler-Lagrange coupling with damping effects: Application to slamming problem", 2006, *Computer Methods in applied Mechanics and Engineering*, 195, pp.110-132
11. M. Souli, A. Ouahsine, and L. Lewin, "ALE formulation for fluid-structure interaction problems", 2000, *Computer methods in applied mechanics and engineering*, 190, pp.659-675
12. E. L. Lee, H. C. Hornig, and J. W. Kury, "Adiabatic expansion of high explosive detonation products",

Lawrence Radiation Laboratory, University of California, 1968, UCRL-50422

13. S. Itoh, H. Hamashima, K. Murata, and Y. Kato, “ Determination of JWL parameters from underwater explosion test” , *Proc. of 12th International Detonation Symposium*, 2002, pp.281-285